Disalignment rates of the neon $2p_5$ and $2p_{10}$ atoms due to helium atom collisions measured at temperatures between 77 and 294 K

H Matsukuma 1, T Shikama and M Hasuo

Department of Mechanical Engineering and Science, Graduate School of Engineering, Kyoto University, Yoshida Hon-machi, Sakyo, Kyoto, 606-8501, Japan
E-mail: hiraku@t04.mbox.media.kyoto-u.ac.jp

1 Author to whom any correspondence should be addressed.

(Abstract)

Using a positive column of helium–neon glow discharge plasma at several temperatures between 77 and 294 K, the disalignment rates of excited neon atoms in the $2p_5$ and $2p_{10}$ (in Paschen notation) levels are measured by a polarization-resolved laser-induced fluorescence technique. For the $2p_{10}$ case, the disalignment rate due to radiation reabsorption is evaluated from the optical thickness of the plasma measured by a self-absorption method, and then is subtracted from the disalignment rate measured. From the slope of the obtained disalignment rate plotted against the helium atom density we determine the rate coefficients due to helium atom collisions. These rate coefficients are compared with the results of quantum multi-channel close-coupling calculations using the modified long-range potentials proposed by Bahrim and Khadilkar (2009 Phys. Rev. A 79 042715) from the original potentials of Hennecart and Masnou-Seeuws (1985 J. Phys. B: At. Mol. Phys. 18 657). Our present experiment agrees excellently with the theory for the $2p_5$ level at any temperatures between 77 and 294 K, and for the $2p_{10}$ state only at 294 K. Below 294 K, the experimental rate coefficients for the $2p_{10}$ state show a more rapid decrease with the decrease in temperature than the theory predicts.

1. Introduction

The analysis of inter- and intra-multiplet transitions induced in atom–atom collisions within the framework of the molecular theory has been discussed in many papers (e.g. [1]) and textbooks (e.g. [2]). In order to test the accuracy of the molecular potentials between colliding atoms proposed in theoretical models, several elementary processes have been investigated experimentally. In particular, the multipole relaxations of the polarized atoms due to atom–atomcollisions give a good indication about the accuracy of the anisotropic molecular potentials [3–5].

The rate coefficients of the disalignment (which is defined as the relaxation of the normalized alignment $\rho^2{}_0/\rho^0{}_0$) of the neon atoms excited on the $2p_2$ and $2p_7$ states (in Paschen notation) of the $2p^53p$ configuration due to helium atom collisions have been already determined in a temperaturecontrolled discharge cell at temperatures between 15 and 600 K with the polarization-resolved laser-induced fluorescence (LIF) technique in [4, 6]. A partial energy diagram of the $2p^53p$ configuration is shown in figure 1 together with that of the $2p^53s$ configuration. The $2p_2$ and $2p_7$ states have the total angular momentum quantum number J = 1, which are highlighted by the thick lines in

figure 1 together with other states having J = 1. In the definition of the atomic disalignment ρi j represents the irreducible tensor components of the atomic density matrix, or the components of the state multipoles (for more details, see [7]). The experimental results were compared with those from the quantum calculations of the disalignment cross sections [6, 8] based on the model potentials of Hennecart and Masnou-Seeuws for the Ne*($2p^5 3p$)–He system [9]. Above 77 K, the theory and experiment are in agreement while the experimental values show a more rapid decrease with the decrease in the temperature from40 to 15Kthan the theoretical results [6].

In the early 1970s, Carrington et al have investigated the alignment destruction of the Ne*($2p_i$; J = 1) atoms, where i = 2, 5, 7 and 10, due to helium atom collisions based on the measurements of Hanle signals at temperatures of 85, 315 [10] and 870 K [11]. The alignment destruction includes both the inter-multiplet and intra-multiplet transitions and it is a different elementary process from the disalignment of atoms measured with the LIF method, as proved in [12]. The latter process includes only the intra-multiplet transitions between the magnetic sublevels. In [11] they concluded that, however, they were not able to measure the alignment destruction of the $2p_{10}$ atoms because of the weak Hanle signals at 85 and 870 K.

Since there were noticeable differences between the experimental results of the disalignment [6, 8] and alignment destruction [10], and the calculated values using the potentials taken from[3], Bahrimand Khadilkar have modified the model potential for the Ne*($2p^5 3p$)–He system by adding the static dipole polarizabilities of the Ne*($2p_i$; J = 1) atoms, where i = 2, 5, 7 and 10, and calculated the disalignment rate coefficients and the effective cross sections for the alignment destruction of these atoms due to helium atom collisions. The disalignment rates reported in [5] show excellent agreement with the experimental data for the disalignment of the $2p_7$ atoms at temperatures between 15 and 600 K, while for the $2p_2$ atoms the agreement is shown only at temperatures between 77 and 600 K (shown in figure 2). The calculations of the energy-averaged cross section for the alignment destruction agree with the experimental data [10] for the $2p_2$, $2p_5$, $2p_7$ atoms at 85 and 315 K [5] and $2p_{10}$ atoms at 315 K [14].

In [5], Bahrim and Khadilkar predicted that an additional dipole polarizability has a larger effect on the disalignment rate coefficient of the $2p_5$ state than those of the other $2p_i$ (i = 2, 7 and 10) states. Matsukuma et al measured the disalignment rate coefficient of the $2p_5$ level due to helium atom collisions at 77 and 292 K [15]. Their result for the $2p_5$ case is much closer to the theoretical value calculated based on the modified potentials [5] than that based on the potentials from [3] with quantum

many-channel close-coupling calculations explained in section 4 of [14]. On the other hand, Bahrim and Khadilkar have shown that the disalignment rate coefficient for the $2p_{10}$ case is not sensitive to the inclusion of the dipole polarizability of the Ne*($2p_{10}$) atom [5]. However, no experimental data of disalignment rate coefficient for the $2p_{10}$ state are available yet.

In this paper we report our measurements of disalignment rates of the neon $2p_{10}$ atoms due to helium atom collisions using the LIF method at temperatures between 77 and 294 K. We also report experimental results for the neon $2p_5$ atoms between 77 and 294 K. Our measurements are compared with the theoretical rate coefficients in [5].

2. Experiment

2.1. LIF measurement

Figure 3(a) shows a schematic diagram of the experimental setup for the LIF measurement. A temperature-controlled glow discharge cell is made of fused quartz and its structure is shown in figure 2 of [16]. The discharge tube is composed of a cylindrical discharge channel (5 mm inner diameter and 190 mm length), its surrounding layer for the temperature control of the channel and a vacuum layer for the thermal isolation from the outside. The discharge channel is filled with a mixture of neon and helium gases. For the temperature of the discharge channel to be set at 77 K, the temperaturecontrolled layer is filled with liquid nitrogen. We set the temperature between 77 and 240 K by controlling a flow rate of nitrogen gas cooled by liquid nitrogen. At 294 K, the temperature-controlled layer is exposed to air at room temperature. The temperature of the channel is measured with a thermocouple attached to the outside wall of the channel. Fluctuations of the measured temperature are less than 2 K during a series of measurements. The gas pressure is measured with a ceramic capacitance manometer (ULVAC, CCMT-100A) at room temperature. The dc discharge current is 0.70 mA. We define the (x, y, z) coordinate as shown in figure 3(a).

The excitation light source is a dye laser (ELTO, LT1233) pumped by the second harmonic of a pulsed YAG laser (Spectra Physics, GCR-100) light. A laser light pulse at the wavelength $\lambda = 743.9$ nm excites the $2p_{10}$ ($J = 1$) atoms and that at $\lambda = 626.6$ nm excites the $2p_5$ ($J = 1$) atoms from the metastable $1s_3$ ($J = 0$) atoms generated in the discharge. The respective active media of the dye laser are LDS 751 and DCM dissolved in methanol. The pulse duration of the laser light is 5 ns (FWHM) and the pulse repetition rate is 50 Hz. We detect a small part of the laser light by a PIN photo diode (Hamamatsu, S3883) and use its output as the monitor of the excitation laser light

energy and also as the trigger of a digital oscilloscope (Agilent, DSO5054A). The main part of the laser light is linearly polarized along the z direction by a Glan–Thompson prism located in front of the discharge cell's window. The diameter of the light beam is about 1 mm at the position of the observation. The reflected beam at the exit window is attenuated by the light dump.

The fluorescence is observed through the slit on the side wall of the discharge channel and the viewing window along the direction perpendicular to the laser beam in the plane of figure 3(a). The direct fluorescence of the $1s_4$ (J = 1) ← $2p_{10}$ (J = 1) (λ = 724.5 nm) or the $1s_2$ (J = 1) ← $2p_5$ (J = 1) (λ = 671.7 nm) transition is observed with a photomultiplier tube (Hamamatsu, H6780-02) through an analysing polarizer and a monochromator (Nikon, G-250). Thus we measure separately the intensities of the π - and σ -components. The entrance slit of the monochromator is parallel to the discharge channel axis. The width and the height of the entrance slit are 0.5 mm and 5 mm, respectively, those of the exit slit are 1.0 mm and 20 mm, respectively. The temporal change of the output signal of the photomultiplier is recorded by a digital oscilloscope with a time resolution of 2 ns. These digital signals are accumulated over laser excitation pulses. The number of the accumulations is 1024.

In order to determine the relative sensitivity of the π - to the σ -polarization component in our detection system, we polarize the excitation light to the x direction. In this case, the fluorescence intensity is independent of its polarization direction around the x axis. From measurements of the fluorescence intensities for each polarized component, the relative sensitivities (σ -component/π -component) are determined to be 0.426 and 0.606 for the wavelengths of 724.5 and 671.7 nm, respectively.

Since the spectral line width of the excitation laser light is sufficiently broad compared to the absorption line widths, the velocity distributions of the excited atoms in the $2p_{10}$ and $2p_5$ levels are assumed to be identical to that of the $1s_3$ atoms. The temperature of the $1s_3$ atoms is confirmed to be virtually equal to the wall temperature of the discharge channel from the measurement of the absorption profiles of the $1s_3$ (J = 0) → $2p_7$ (J = 1) transition line (λ = 653.3 nm) by use of a single-mode CW diode laser [4, 16].

2.2. Self-absorption measurement

As discussed in the next section, quantitative estimation of the radiation reabsorption for the $2p_{10}$ emissions in the plasma is important. For this purpose, we observe the self-absorption of the plasma [16, 17] for the transition lines shown in figure 4. In figure 3(b) we show the schematic diagram of the self-absorption experimental setup. We

observe the emission lines from the dc discharge plasma with the same monochromator, photomultiplier tube and oscilloscope without the analysing polarizer. The width and the height of the entrance and exit slits are 0.03 mm and 5 mm, respectively. We cut the excitation laser light and place a concave mirror which has the same focal length of 75 mm as that of the collection lens on the opposite side of the discharge tube to the observation direction. The light from the discharge plasma through the slit of the discharge channel wall is reflected back and focused by this mirror on the plasma itself. We measure the spectrum of each 1si (i = 2, 3, 4 and 5) ← $2p_{10}$ emission line by scanning the wavelength with and without the concave mirror. We evaluate the areas of each spectrumas the emission line intensities. As a measure of the optical thickness of the plasma to the transition line, we define the line absorption, α, as

$$\alpha = 1 - \left(\frac{I_2 - I_1}{I_1}\right), \qquad (1)$$

where I_1 is the observed emission line intensity without the mirror and I_2 is that with the mirror. The transmittance of the windows and the reflectance of the mirror are taken into account. We observe emission lines under such conditions that the transition line has sufficiently small optical thickness, so that the line absorption should be virtually null. From the measured intensities obtained with and without the mirror, we determine the effective reflection-transmission coefficient of the mirror-windows combination. The coefficient is found to be typically 43%and it slightly depends on thewavelength. By using these coefficient values, we determine the line absorption of the four emissions shown in figure 4 under all the discharge conditions for the LIF measurements.

3. Results

3.1. Analysis of the LIF measurement

Figure 5(a) shows an example of the temporal evolution of the fluorescence intensities with the π - and σ -components resolved. The intensities I_π (t) and I_σ (t) are calibrated with the relative sensitivity. Since the excitation is performed with the π -polarized light in the J = 0 to J = 1 transition, the initial population of the upper level is produced only in the MJ = 0 sublevel, where MJ is the magnetic quantum number. During the lifetime of the upper level, the excitation transfer from the M_J = 0 sublevel to M_J = +1, − 1 sublevels may take place due to neon–helium, neon–neon and neon–electron collisions and radiation reabsorption whose contributions to the disalignment rate are discussed

in sections 3.2.1 and 3.2.2. As a consequence, the π -component appears in the fluorescence. After the cessation of the excitation laser light pulse, the coupled rate equations for the sublevel populations in the upper $2p_i$ levels are

$$\begin{aligned} \frac{dn_0(t)}{dt} &= -(2k+\gamma)n_0(t) + 2kn_1(t) \\ \frac{dn_1(t)}{dt} &= kn_0(t) - (k+\gamma)n_1(t), \end{aligned} \qquad (2)$$

where k is the excitation transfer rate between the $M_J = 0$ and $M_J = 1$ or -1 sublevels, γ is the depopulation rate of the 2pi level and n0 and n1 are the populations of the $M_J = 0$ and $M_J = 1$ or -1 sublevels, respectively. The intensities of the polarized components of the fluorescence are

$$\begin{aligned} I_\sigma(t) &= C\tfrac{1}{2}[n_0(t) + n_1(t)] \\ I_\pi(t) &= Cn_1(t), \end{aligned} \qquad (3)$$

where C is a constant that depends on the detection efficiency of the fluorescence and Einstein'sA coefficient of the observed transition, which is the same for all the magnetic sublevels of the same 2pi level. We define the longitudinal alignment for the emitted radiation as

$$A_L(t) \equiv \frac{I_\pi(t) - I_\sigma(t)}{I_\pi(t) + 2I_\sigma(t)} = -\frac{1}{2}\frac{n_0(t) - n_1(t)}{n_0(t) + 2n_1(t)}. \qquad (4)$$

The second equality in equation (4) is easily found by substitution of the π - and σ -components from equation (3). Figure 5(b) shows the temporal evolution of the longitudinal alignment obtained fromthe fluorescence intensities presented in figure 5(a). Using equation (2), one can find the temporal evolution of A_L expressed as

$$A_L(t) = -\frac{1}{2}\frac{n_0(0) - n_1(0)}{n_0(0) + 2n_1(0)}\exp[-3kt]. \qquad (5)$$

We may determine the relaxation time, (3 k)− 1, which is due to the intra-multiplet transitions within the same $2p_i$ (J = 1) level and corresponds to the disalignment rate [13], from the slope ln [− AL(t)].

The longitudinal alignment in figure 5(b) shows a single exponential decay with time. The disalignment rate coefficient is determined by fitting the experimental data points with equation (5). The result of the least squares fitting is indicated by the full line in figure 5(b).

3.2. Disalignment rate as a function of the helium atom density

3.2.1. Disalignment of the $2p_{10}$ state. Figure 6(a) shows the disalignment rate of the $2p_{10}$ state of neon as a function of the helium atom density at 77, 135, 180, 240 and 294 K. The uncertainty of each data point is within the size of the symbols in the figure. The partial pressure of the neon gas is set to be constant at about 0.09 Torr over the same temperature measurements.

Since the electron density is about 10^{16} m^{-3} in our experimental conditions [18], the disalignment rate due to electron collisions is about 10^4 s^{-1} for the $2p_2$ case [19], which is two or more orders of magnitude smaller than the disalignement rate in figure 6(a). We assume that the disalignment due to electron collisions can be neglected for the other $2p_i$ states. The disalignment rates due to neon atom collisions at 0.09 Torr between 77 and 294 K are estimated to be less than 2×10^5 s^{-1} from the results of other experiments which we have performed[2].

Figure 7 shows the line absorptions at 77 K, where the measured disalignment rates show a significant deviation from the linear dependence on the helium atom density. The line absorption for the $1s_5 \leftarrow 2p_{10}$ emission is the largest and its increasing tendency below the helium atom density of 1.5×10^{24} m^{-3} is similar to that of the disalignment rate in figure 6(a). Due to the small emission intensity of the $1s_2 \leftarrow 2p_{10}$ emission, the error bars and the scatter of the line absorption for the emission are much larger than those for the other emissions.

We evaluate the disalignment rate due to the radiation reabsorption with a Monte Carlo simulation program using the measured values of the self-absorption and then subtract it fromthe measured disalignment rate. The method is explained in detail in [16]. Here we neglect the contribution of the radiation reabsorption for the emission lines from the $2p_{10}$ to $1s_2$ states because the accuracy of the line absorption for the emission is not enough as mentioned above and the line absorption for the emission itself is thought to be smaller than that for the $2p_{10}$–$1s_4$ transition line because

[2] We estimated upper limits of the disalignment rate due to neon atom collisions to be 6.0×10^4, 1.4×10^5, 1.6×10^5, 1.9×10^5 and 1.4×10^5 s^{-1} for 77, 135, 180, 240 and 294 K, respectively, with a pure neon gas discharge.

Einstein's A coefficient of the former transition is smaller as shown in figure 4 and the population in the $1s_2$ state is smaller than that in the $1s_4$ state in a similar discharge condition [16]. Figure 6(b) shows the disalignment rate against the helium atom density after this correction has been made. The full lines are the results of the linear fit based on the least-squares method with a null intercept. Finally, we determine the disalignment rate coefficient of the $2p_{10}$ state of neon for the collisions with the ground-state helium atom from the slope of the linear fit.

In the simulation, we assume that the radial distribution of the atom density in the lower levels in the discharge channel is represented by the zeroth-order Bessel function based on the result of the LIF measurement for the lower level spatial distribution in a similar glow discharge tube [16]. In [20], however, it is pointed out that the radial spatial profile of the plasma is different from a Bessel function profile due to the radial dependence of energy distribution of electrons. In order to confirm the effect of the shape of the radial distribution on the simulation results, we performed the simulation under a condition of uniform density distribution as an extreme case. We found that the differences between these two cases are smaller than the experimental errors.

In figure 6(a) the contributions of radiation reabsorption are larger in lower temperature and lower helium atom density cases. The reasons are as follows. At a low temperature, the disalignment rate due to helium atom collisions is small. In addition, the smaller Doppler width at a lower temperature gives the larger optical thickness of the emission line than that at a high temperature even at the same lower level populations. Furthermore, the population in the metastable $1s_5$ state may become larger in lower helium atom density situations because of the smaller depopulation rate due to atomic collisions. The $1s_5$ state is the dominant lower level, so that the larger population leads to the larger contribution to radiation reabsorption.

3.2.2. Disalignment of the $2p_5$ state. Figure 8 shows the disalignment rate of the $2p_5$ state of neon as a function of the helium atom density at 77, 135, 180, 240 and 294 K, which is derived from the LIF measurement without the separation of the effect of radiation reabsorption. The uncertainty of each data point is within the size of the symbols. In the experiment we fixed the partial pressure of neon gas at 0.05 Torr.

As discussed for the $2p_{10}$ state, the disalignment rate due to electron collisions is negligible. The disalignment rate due to neon atom collisions is estimated to be less than $1.5 \times 10^6\ s^{-1}$ for the $2p_5$ state at the temperatures between 77 and 294 K [15]. Since we keep the neon density constant for all helium densities for each temperature,

the disalignment rate due to neon atom collisions is constant and contributes to the intercept. We note that the disalignment rate coefficient for the $2p_5$ state at low temperatures is about one or two orders of magnitude larger than that for the $2p_{10}$ state. In the $2p_5$ case, the correction of the disalignment rate due to radiation reabsorption seems to have a similar magnitude to the $2p_{10}$ state or is rather smaller than that for the $2p_{10}$ case. We assume that the correction due to the radiation reabsorption is constant and contributes to the intercept. Therefore, we determine the disalignment rate coefficient of the $2p_5$ state of neon due to the ground-state helium atoms from the slope of each linear fit.

4. Discussion

The disalignment rate coefficients for the Ne□($2p_{10}$) + He and Ne□($2p_5$) + He collisions as a function of temperature are shown in figure 2. Excellent agreement between theory [5] and experiment for the $2p_5$ state is observed. In figure 2(a) we also show the measurements of the disalignment rate coefficient reported in [15]. The small deviation of the data from [15] may be caused by a fitting error due to the lack of enough data points in figure 4 of [15].

The experimental disalignment rate coefficients of the $2p_{10}$ state are smaller than those of the other 2pi (i = 2, 5 and 7) states as predicted in [5]. However, the rates for the $2p_{10}$ state show a more rapid decrease with decreasing temperature below 294 K than the theory [5] predicted, and also a simple temperature dependence: $T^{2.2}$. At the present stage the origin of the discrepancy between the quantum calculation [5] and our experiment is not clear. Recent studies performed by Bahrimsuggest that the quantumintra-multiplet cross sections at collision energies below 10 meV (which is a region with significant contribution to the rate coefficients below 140 K due to the energy distribution of atoms) should be linearly extrapolated towards the zero energy [21], similar to the $2p_2$ case discussed in section 6 of [22].

Acknowledgments

We are grateful to Professor Cristian Bahrim for encouraging us and sharing the theoretical data, as well as for his comments to the manuscript. This work was partly supported by Grantin- Aid for Scientific Research (B) (no 21340170).

References

[1] Mies F H 1973 Phys. Rev.A 7 942 Manders M P I, Driessen J P J, Beijerinck H C W and Verhaar B J 1988 Phys. Rev.A 37 3237 Hickman A P 1997 Int. Rev. Phys. Chem.16 177

[2] Nikitin E E and Umanskii S Ya 1984 Theory of Slow Atomic Collisions (Berlin: Springer)

[3] Bahrim C, Kucal H and Masnou-Seeuws F 1997 Phys. Rev.A 56 1305

[4] Wakabayashi T, Yamamoto A, Yaneda T, Furutani T, Hishikawa A and Fujimoto T 1998 J. Phys. B: At. Mol. Opt. Phys. 31 341

[5] Bahrim C and Khadilkar V V 2009 Phys. Rev.A 79 042715

[6] Seo M, Shimamura T, Furutani T, Hasuo M, Bahrim C and Fujimoto T 2003 J. Phys. B: At. Mol. Opt. Phys. 36 1885

[7] Omont A 1977 Prog. Quantum Electron. 5 69

[8] Bahrim C, Kucal H, Dulieu O and Masnou-Seeuws F 1997 J. Phys. B: At. Mol. Opt. Phys.30 L797

[9] Hennecart D and Masnou-Seeuws F 1985 J. Phys. B: At. Mol. Phys. 18 657

[10] Carrington C G and Corney A 1971 J. Phys. B: At. Mol. Phys. 4 869

[11] Carrington C G, Corney A and Durrant A V 1972 J. Phys. B: At. Mol. Phys.5 1001

[12] Fujimoto T and Matsumoto S 1988 J. Phys. B: At. Mol. Opt. Phys. 21 L267

[13] Nimura M, Hasuo M and Fujimoto T 2004 J. Phys. B: At. Mol. Opt. Phys. 37 4647

[14] Khadilkar V V and Bahrim C 2010 J. Phys. B: At. Mol. Opt. Phys. 43 235209

[15] Matsukuma H, Bahrim C and Hasuo M 2009 J. Plasma Fusion Res. Ser. 8 169

[16] Seo M, Nimura M, Hasuo M and Fujimoto T 2003 J. Phys. B: At. Mol. Opt. Phys.36 1869

[17] Nimura M, Imagawa T, Hasuo M and Fujimoto T 2005 J. Quant. Spectrosc. Radiat. Transfer 96 547

[18] Uetani Y and Fujimoto T 1984 Opt. Commun.49 258 Uetani Y and Fujimoto T 1985 Opt. Commun. 55 457 (erratum)

[19] Hirabayashi A, Nambu Y, Hasuo M and Fujimoto T 1988 Phys. Rev.A 37 83

[20] Alves L L, Gousset G and Vallee S 2003 IEEE Trans. Plasma Sci. 31 572

[21] Bahrim C 2010 private communication

[22] Bahrim C and Khadilkar V V 2008 J. Phys. B: At. Mol. Opt. Phys. 41 035203

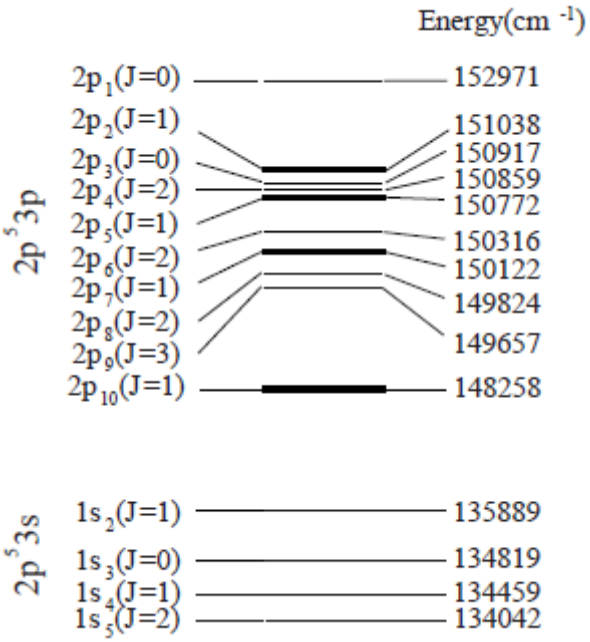

Figure 1. A partial energy level diagram of the $2p^5 3s$ and $2p^5 3p$ configurations of neon atoms. The indicated energies are those from the ground state.

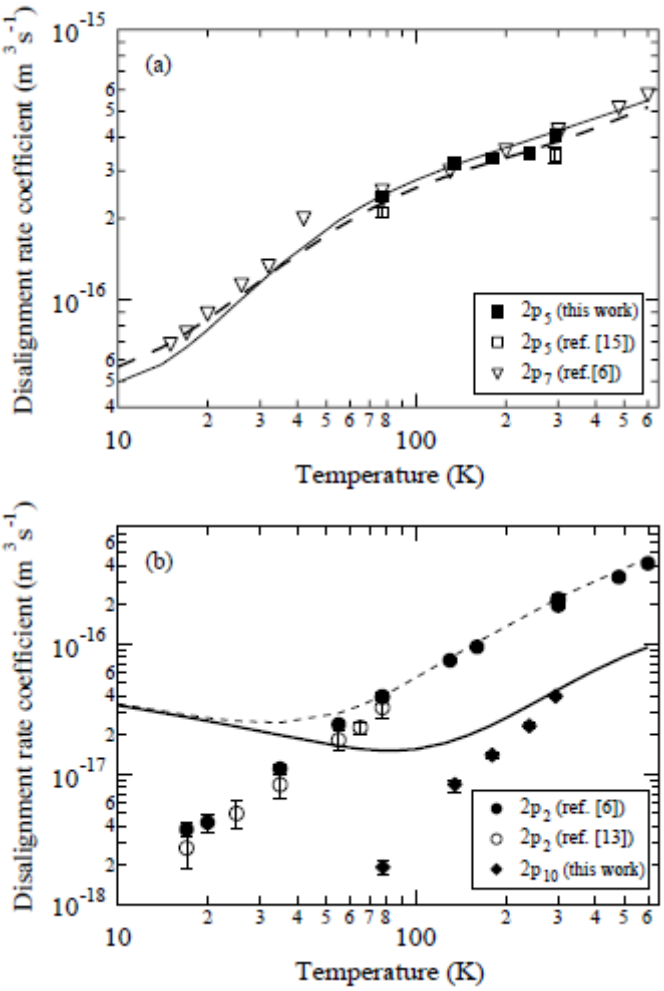

Figure 2. The disalignment rate coefficient for the Ne*(2p$_i$) + He (i = 2, 5, 7 and 10; J = 1) collisions as a function of temperature. (a) 2p$_5$ and 2p$_7$. (b) 2p$_2$ and 2p$_{10}$. Theoretical curves are also shown: 2p$_2$ (thin dased), 2p$_5$ (thin full), 2p$_7$ (thick dashed) and 2p$_{10}$ (thick full).

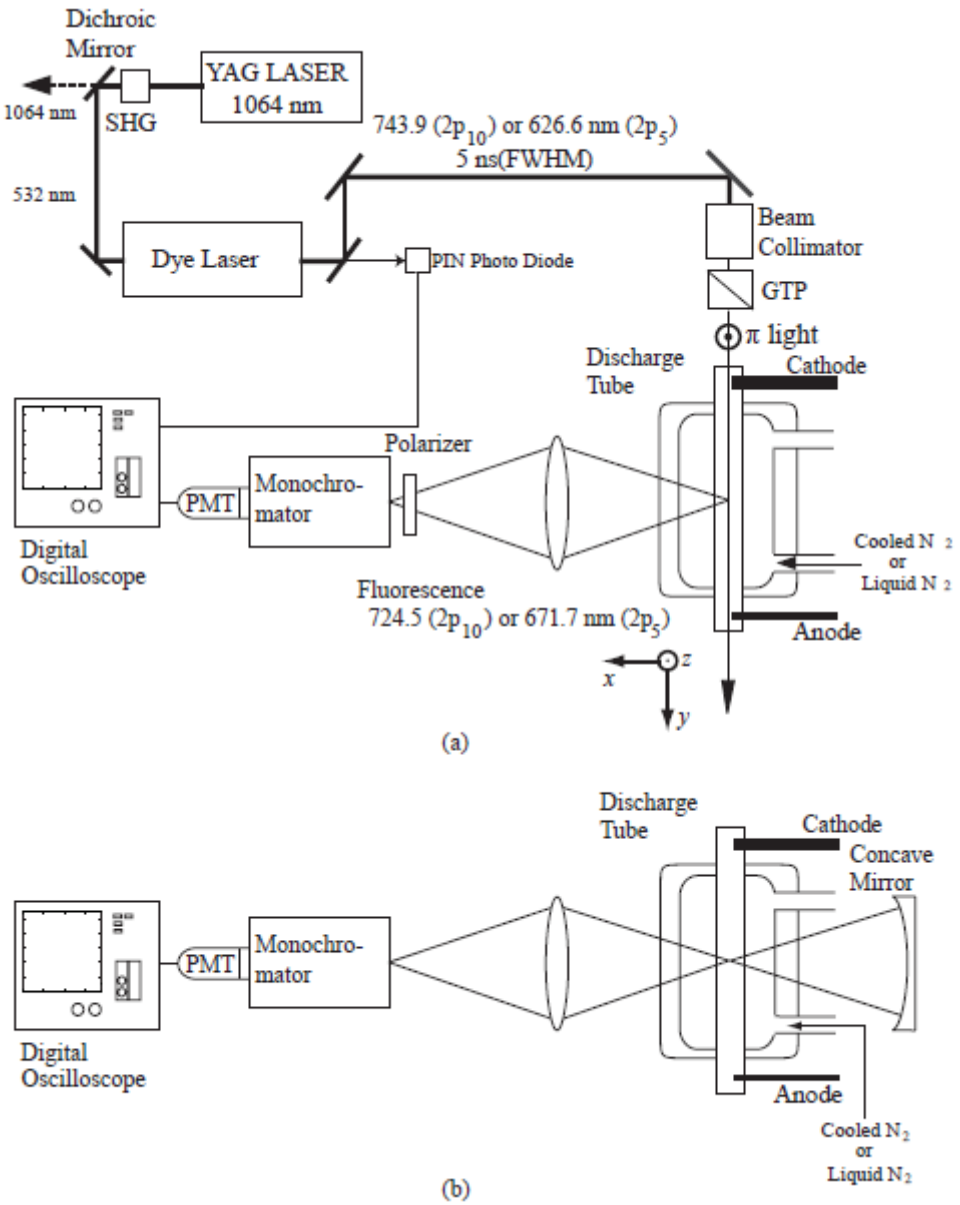

Figure 3. Schematic diagrams of the experimental setups. SHG: second harmonic generator, GTP: Glan–Thompson prism and PMT: photomultiplier tube. (a) LIF measurement. (b) Self-absorption measurement.

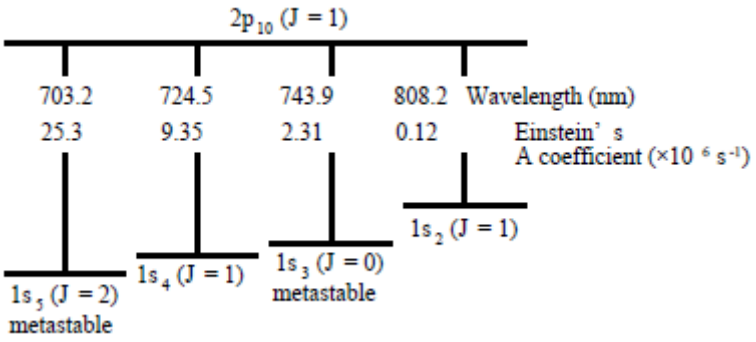

Figure 4. A partial energy level diagram relevant to the $1s_i$–$2p_{10}$ (i = 2, 3, 4 and 5) transitions. The wavelengths and transition probabilities are shown.

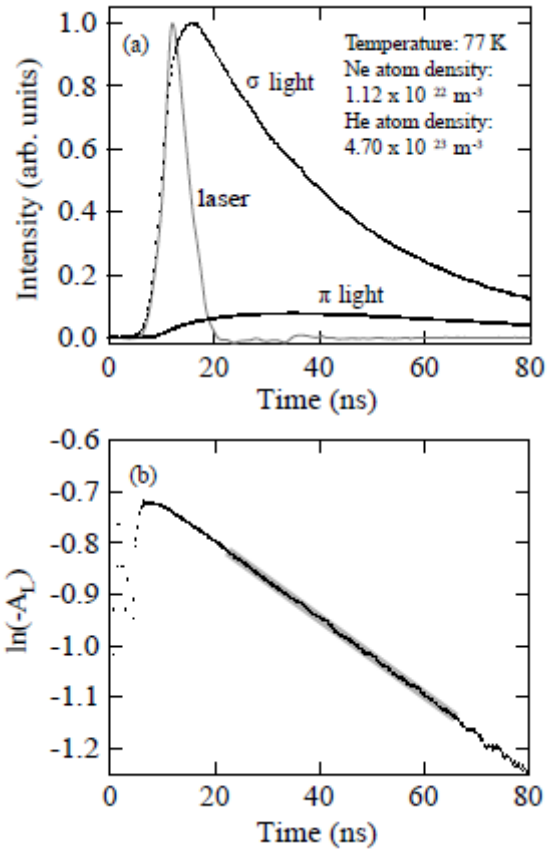

Figure 5. An example of the observed temporal developments for (a) the fluorescence $1s_4$ (J = 1) ← $2p_{10}$ (J = 1) (λ = 724.5 nm) intensities of the π - and σ -components (dots) and the temporal development of the laser pulse (curve) and (b) the longitudinal alignment.

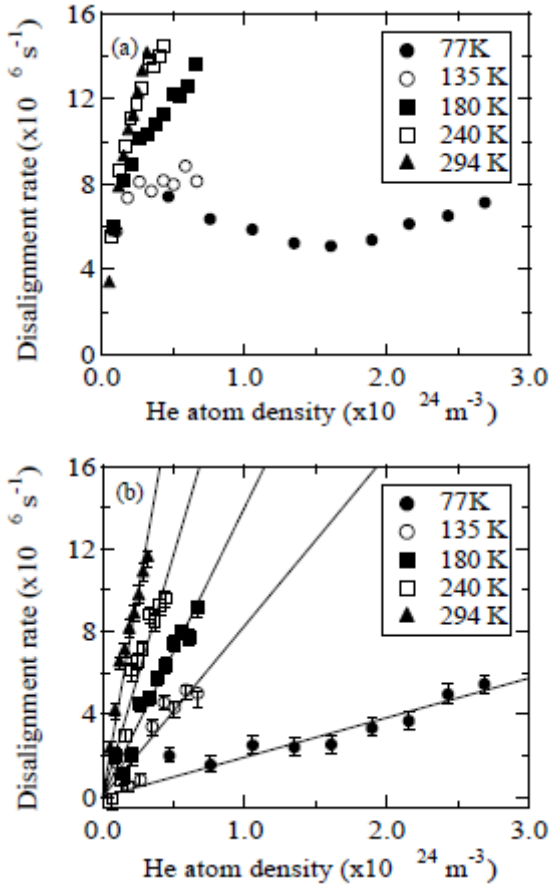

Figure 6. Experimental values for the disalignment rate of the $2p_{10}$ state of neon as a function of the helium atom density. In (a) the disalignment rates are determined from the linear fit like figure 5(b) (the experimental error bars are within the size of the symbols), while in (b) the effect of the radiation reabsorption is separated from (a). The full lines in (b) show the results of the linear fit within the least-squares method with the null intercept for each temperature.

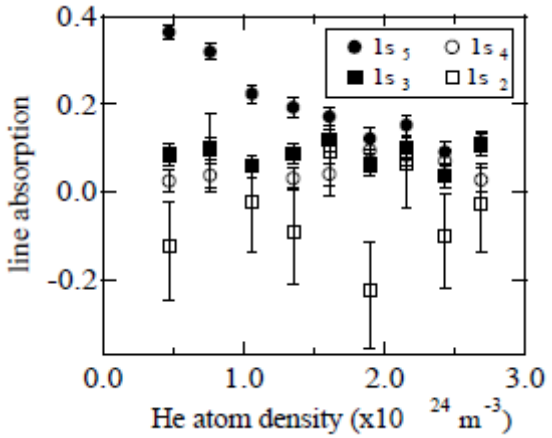

Figure 7. The line absorptions of the emission from the $2p_{10}$ to $1s_5$ (closed circles), $1s_4$ (open circles), $1s_3$ (closed squares) and $1s_2$ (open squares) states as a function of the helium atom density at 77 K.

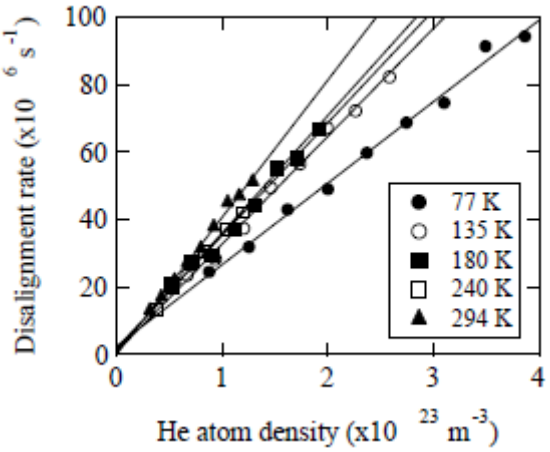

Figure 8. Experimental values for the disalignment rate of the $2p_5$ state of neon as a function of the helium atom density. The full lines are the results of the linear fit within the least-squares method for each temperature. The experimental error bars are within the size of the symbols.